Available online at www.sciencedirect.com
ScienceDirect
Journal of the European Ceramic Society 30 (2010) 799–804
www.elsevier.com/locate/jeurceramsoc

Technical note

Thermal conductivity of plasma sprayed $Sm_2Zr_2O_7$ coatings

Jianhua Yu [a,b,c], Huayu Zhao [a,b], Shunyan Tao [a,b,*], Xiaming Zhou [a,b], Chuanxian Ding [a,b]

[a] *The Key Laboratory of Inorganic Coating Materials, Chinese Academy of Sciences, Shanghai 200050, China*
[b] *Shanghai Institute of Ceramics, Chinese Academy of Sciences, Shanghai 200050, China*
[c] *Graduate School of the Chinese Academy of Sciences, Beijing 100039, China*

Received 16 April 2009; received in revised form 6 September 2009; accepted 10 September 2009
Available online 8 October 2009

Abstract

Rare-earth zirconates with a pyrochlore structure have been developed for potential application in thermal barrier coating systems to further improve the performance and durability of gas turbines. The $Sm_2Zr_2O_7$ (abbreviated as SZ) powder was synthesized by solid state reaction and then deposited by air plasma spraying. The phase stability, microstructure and thermal conductivity of SZ and 8 wt% Y_2O_3 stabilized zirconia (8YSZ) coatings were investigated. The X-ray diffraction results indicated that the crystal structure of the as-sprayed SZ coatings was defect-fluorite, and after heat treating at 1200 °C for 50 h, it started to transform to pyrochlore, and the content of pyrochlore increased with increase in temperature of the heat treatment. The thermal conductivities of SZ coatings were significantly lower than those of 8YSZ coatings before and after heat treatments, which increased considerably after heat treatments compared to the as-sprayed states for both coatings due to sintering effects.

Keywords: Plasma spraying; Thermal conductivity; $Sm_2Zr_2O_7$; Thermal barrier coating

1. Introduction

Thermal barrier coatings (TBCs) have been widely used in hot-section metal components of advanced gas turbines to improve the reliability and durability as well as the efficiency of engines.[1–3] Partially stabilized zirconia containing 7–8 wt% Y_2O_3 (8YSZ) deposited by atmospheric plasma spraying (APS) or electron-beam physical vapor deposition (EB-PVD) is presently used as the typical TBCs in gas turbines mainly owing to its relatively high thermal expansion coefficient and low thermal conductivity.[4,5] However, the application of 8YSZ has been limited due to the accelerated sintering and phase transformations during long-term service above 1200 °C.[6] In the next generation of engines, a higher gas temperature is expected to further improve power-to-weight ratio, therefore an exploration of new TBCs candidate materials is needed to provide better thermal insulation and higher temperature stability than 8YSZ coating, thus offering higher engine efficiency and longer durability.

The thermal conductivity of material will be reduced by point defects including vacancies and substituted atoms which are strong phonon scatterers. The larger the difference in mass between the solvent and solute atoms, the lower the thermal conductivity will be obtained.[7] A number of materials with low thermal conductivity have been identified by calculating the minimum thermal conductivity,[8] especially, the rare-earth zirconates – $Ln_2Zr_2O_7$ (Ln – La, Nd, Sm and Gd) with a pyrochlore structure have attracted great attention because they are refractory up to temperatures in excess of 1500 °C and thermally stable. As another critical requirement for TBCs' durability, the thermal expansion coefficient (TEC) of the candidate material should be larger than 9×10^{-6} °C^{-1} to reduce the mismatch between the ceramic and the superalloy substrate.[9] The thermal expansion of any material is directly related to its crystal structure and bonding. With the similar crystal structure, the decrease in the ionic bond strength of Ln–O will be beneficial for the dilation and for increasing TEC, and the bond energy of Sm–O (5.8 eV) is the lowest among Ln–O (Ln – La, Nd, Sm and Gd).[10]

Recently, the thermal conductivity and thermal expansion of pyrochlore zirconates have been investigated, and the thermal conductivity of $Sm_2Zr_2O_7$ (abbreviated as SZ) was the lowest which was similar with that of $Gd_2Zr_2O_7$, while the TEC of SZ was higher than that of $Gd_2Zr_2O_7$.[11] In addition, the relationships between the deposition conditions and the

* Corresponding author at: The Key Laboratory of Inorganic Coating Materials, Chinese Academy of Sciences, Shanghai 200050, China.
Tel.: +86 21 52414101; fax: +86 21 52413903.
E-mail address: shunyantao@mail.sic.ac.cn (S. Tao).

0955-2219/$ – see front matter © 2009 Elsevier Ltd. All rights reserved.
doi:10.1016/j.jeurceramsoc.2009.09.010

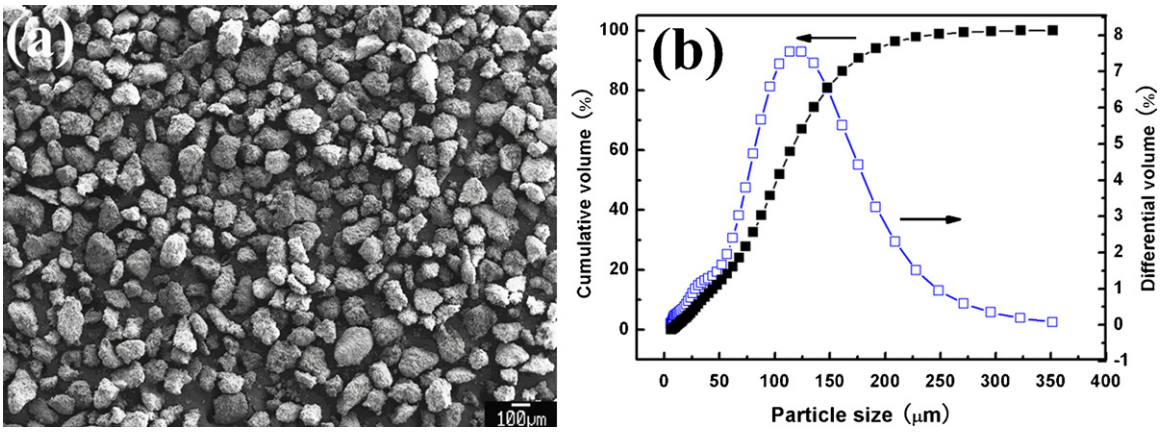

Fig. 1. (a) Morphology and (b) particle size distribution of $Sm_2Zr_2O_7$ powder for plasma spraying.

coating composition, structure, texture, pore morphology, and thermal conductivity of SZ coatings deposited by electron-beam directed-vapor deposition have been investigated.[12] However, few reports on the properties of plasma sprayed SZ coatings have been published.

In this work, SZ powder and coatings were prepared. The crystal structure, phase stability, and thermal conductivity of SZ coatings were investigated. As a comparison, 8YSZ coatings were prepared under the same conditions, and the thermal conductivity was studied.

2. Experimental procedure

2.1. Materials and preparation

SZ powder was synthesized by solid state reaction. Sm_2O_3 (≥99.9%, Beijing Founde Star Science & Technology Co., Ltd.) and ZrO_2 (≥99.7%, Sinopharm Chemical Reagent Co., Ltd.) powders were used as starting materials. The oxide powders were heat treated at 800 °C for 2 h before weighing in order to remove absorbed water and carbon dioxide in air firstly. An ethanol-based suspension of the raw materials was mixed in the stoichiometric ratios and was ball milled for 12 h with zirconia balls and then dried at 80 °C for 12 h. The resulting mixture was calcined at 1550 °C for 5 h to obtain pyrochlore structure, and then the as-synthesized powder was ground and granulated before plasma spraying. While commercially available Metco 204NS powder was used as a feedstock to deposit 8YSZ coating. The medium sizes (D_{50}) of SZ and 8YSZ powder are 102.2 μm and 56.1 μm, respectively. Fig. 1 represents the morphology and particle size distribution of SZ powder.

The PT-A2000 atmospheric plasma spraying system equipped with an F4-MB plasma gun (Sulzer Metco AG, Wohlen, Switzerland) was applied to deposit SZ and 8YSZ coatings. The feedstock powders were fed with a Twin 10-C System (Plasma-Technick AG, Switzerland) with Ar as a carrier gas. The plasma spraying parameters are shown in Table 1. To obtain free-standing samples used in this work, coatings of about 3 mm thickness was deposited onto an aluminium substrate with Ar and H_2 as plasma primary and auxiliary gases and then it was removed from the substrate by mechanical method.

2.2. Specimens characterization

The phase compositions of the powder and coatings were identified by X-ray diffraction using a Rigaku D/Max2550 Diffractometer with nickel filtered Cu Kα ($\lambda = 0.154056$ nm) radiation at a scan rate of 4°/min. The particle size distribution was explored by Microtrac S3500 Particle Size Analyser (Nikkiso, Japan). The morphologies of the powder and coatings were examined employing an EMPA-8705 QH2 electron probe analyzer (Shimadzu, Tokyo, Japan).

Thermal diffusivity (α) of coatings was measured, using a laser flash method, as a function of specimen temperature in the range from 200 °C to 1200 °C at intervals of approximately 100 °C. The samples for thermal diffusivity measurement were about 10 mm in diameter and 0.8 mm in thickness. Before the measurement a thin carbon layer was coated on the surfaces of the sample to prevent the direct laser beam transmission. Heat flow was perpendicular to the sample surface. The laser flash technique involved heating one side of the sample with a laser pulse of short duration and measuring the temperature rise on the other side with an infrared detector. Thermal diffusivity (α) was determined from the time required to reach half the maximum temperature and a transient heat conduction analysis of a multi-layer body. The measurement was conducted in a vacuum atmosphere for preventing the carbon film from oxidation. For comparison, the thermal diffusivity

Table 1
Plasma spraying parameters.

Parameters	Unit	Value
Arc current	A	600–650
Primary plasma gas Ar	slpm	30–40
Secondary plasma gas H_2	slpm	10–15
Carrier gas Ar	slpm	3.0
Spray distance	mm	100–120
Nozzle diameter	mm	6.0
Powder inject diameter	mm	2.0

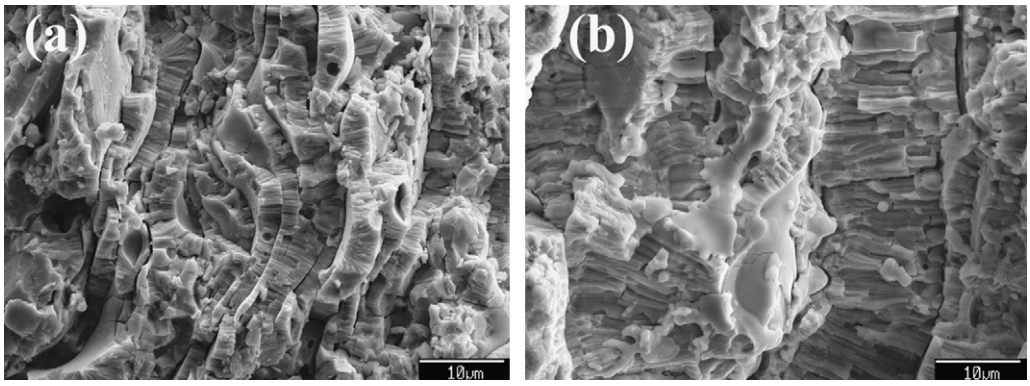

Fig. 2. SEM micrographs of the fracture surface of (a) $Sm_2Zr_2O_7$ and (b) 8YSZ coatings.

of 8YSZ coatings was also measured under the same conditions.

The specific heat capacity (C_p) as a function of temperature was calculated by the Neumann–Kopp rule[13] with the chemical composition of 8YSZ and SZ coatings and the heat capacity data of Sm_2O_3, Y_2O_3 and ZrO_2,[14] and the specific heat capacity of SZ coatings was measured using diamond DSC produced by Perkin Elmer in the temperature range from room temperature to 400 °C to calibrate the calculated values. In this temperature range the measured values were in coincidence with the calculated ones, so the calculated method was used. The thermal conductivity κ is calculated by Eq. (1) with the heat capacity C_p, thermal diffusivity α and density ρ which was measured by the Archimedes method with an immersion medium of deionized water.

$$\kappa = C_p \alpha \rho \quad (1)$$

3. Results and discussion

3.1. Microstructure analysis

The values for the density of SZ and 8YSZ coatings were 5.81 g cm^{-3} and 5.40 g cm^{-3}, corresponding to relative densities of 87.23% and 91.52%, respectively. Fig. 2 shows the cross sectional SEM images of the as-sprayed SZ and 8YSZ coatings, exhibiting a typical layered structure for plasma spraying, which is built up by over-lapping of individual splats aligned predominantly parallel to the substrate surface.[15] Two types of pores are observed in coatings, coarse voids lying along splat boundaries, due to the relatively poor bonding between splats, and fine pores arising from entrapped gas. The literature shows that the pore structure has a strong influence on coating properties, and pores along splat boundaries are more effective in blocking heat conduction than isolated pores.[16]

It is observed (in Fig. 2) that the splat boundaries in 8YSZ coatings are not as clear as that in SZ coatings, and the thicknesses of individual splat in SZ and 8YSZ coatings are about 1–5 μm and 2–15 μm, respectively. Therefore, the splat interface density and layered porosity of $Sm_2Zr_2O_7$ coatings are higher than those of 8YSZ coatings, which would contribute to lowering the thermal conductivity of SZ coatings. The differences in densities and microstructures of plasma sprayed SZ and 8YSZ coatings are ultimately based on the solidification of individual molten droplets which is associated with the conditions of molten, flattening and solidification of the particles in plasma spraying.[17]

The typical microstructure of plasma sprayed SZ coatings heat treated at 1200 °C for 50 h is shown in Fig. 3. It is obvious that most splat interfaces disappeared, the columnar structure exhibited in Fig. 2 is not observed, and the intra-splat globular pores are dominant in the coatings after heat treatment. Therefore, the splat interface density and layered porosity of the coatings after heat treatment are lower than those of as-sprayed

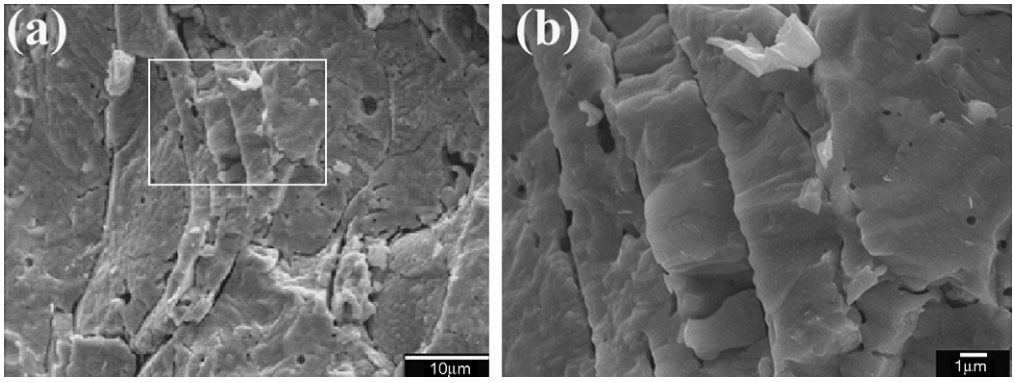

Fig. 3. SEM micrographs of the fracture surface of $Sm_2Zr_2O_7$ coatings heat treated at 1200 °C for 50 h, (b) shows magnified view of framed region in (a).

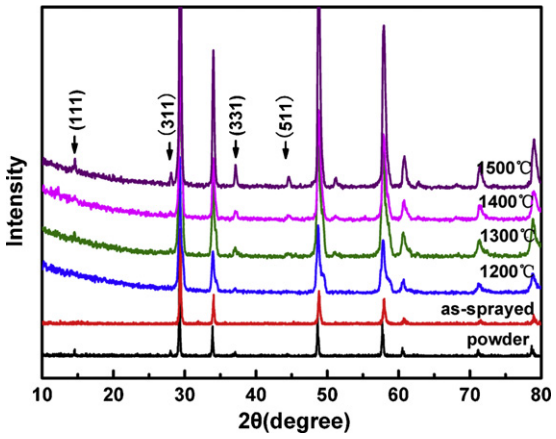

Fig. 4. XRD patterns of $Sm_2Zr_2O_7$ powder, coatings as-sprayed and heat treated at different temperatures for 50 h.

coatings which would contribute to an increase in thermal conductivity.

3.2. Phase stability

The XRD patterns of the SZ powder, coatings as-sprayed and heat treated at different temperatures for 50 h are shown in Fig. 4. Compared the XRD pattern of the as-sprayed coatings with that of the starting powder, it shows that a remarkable change took place during the plasma spraying process. Most of the weak peaks appeared at 2θ values of about 14° (1 1 1), 28° (3 1 1), 37° (3 3 1) and 45° (5 1 1) in the XRD pattern of the starting powder disappeared after plasma spraying. These weak peaks are typical for ordered-pyrochlore structure distinguished from defect-fluorite structure.[18] The phase diagram of ZrO_2–$SmO_{1.5}$ shows that the ordered-pyrochlore structure SZ will transform to defect-fluorite structure when the temperature is above 2000 °C.[19] It was reported[20] that different types of quenching produced different structures of $Gd_2Hf_2O_7$, suggesting a fluorite phase would be obtained by a higher quenching rate. Therefore, defect-fluorite structure SZ phase was maintained due to the high quenching rate (~10^6 °C/s) during the plasma spraying.

Table 2
Chemical compositions of $Sm_2Zr_2O_7$ powder and coatings.

Sample	Sm_2O_3 (wt%)	ZrO_2 (wt%)
Theoretical	58.6	41.4
Starting powder	58.1	41.2
As-sprayed coating	56.3	43

Additionally, small shifts towards the lower d-value of the main peaks of SZ coatings occurred. Chemical compositions of both the starting powder and as-sprayed coatings are listed in Table 2, indicating about 2 wt% Sm_2O_3 is lost during the plasma spraying. It was reported that the BO_6 (B–Zr in SZ) network is much more stable than the AO_8 (A–Sm in SZ) network, which is obtained by the calculation of the Madelung energy of the pyrochlore structure ($A_2B_2O_7$),[21] and this may be contributed to the more loss of Sm_2O_3 than ZrO_2 during plasma spraying. As the ionic radius of Sm^{3+} (0.958 Å) is larger than that of Zr^{4+} (0.72 Å), the more loss of Sm_2O_3 results in the lower d-value shift of the coating.

The comparison between the XRD patterns of SZ coatings before and after heat treatment at different temperatures for 50 h shows that there is no difference except the appearance of the weak peaks. When the coating is heat treated at 1200 °C for 50 h, the pyrochlore structure is partially recrystallized, which is indicated by the appearance of the peak (3 3 1). With increase in treating temperature, the amount of pyrochlore phase is increasing indicated by increase in the number and intensity of the typical peaks. The typical peaks of pyrochlore structure SZ completely appeared in the coating when the coating was heat treated at 1400 °C for 50 h.

3.3. Thermal diffusivity and conductivity

The results of thermal diffusivity measurements and the calculated thermal conductivities of SZ and 8YSZ coatings are illustrated in Fig. 5. The values of thermal diffusivity of the as-sprayed SZ coating slightly decreased with increase in temperature up to 700 °C and then increased with further temperature rise, and the thermal diffusivity of the as-sprayed 8YSZ coating initially decreased below 500 °C where the curve sug-

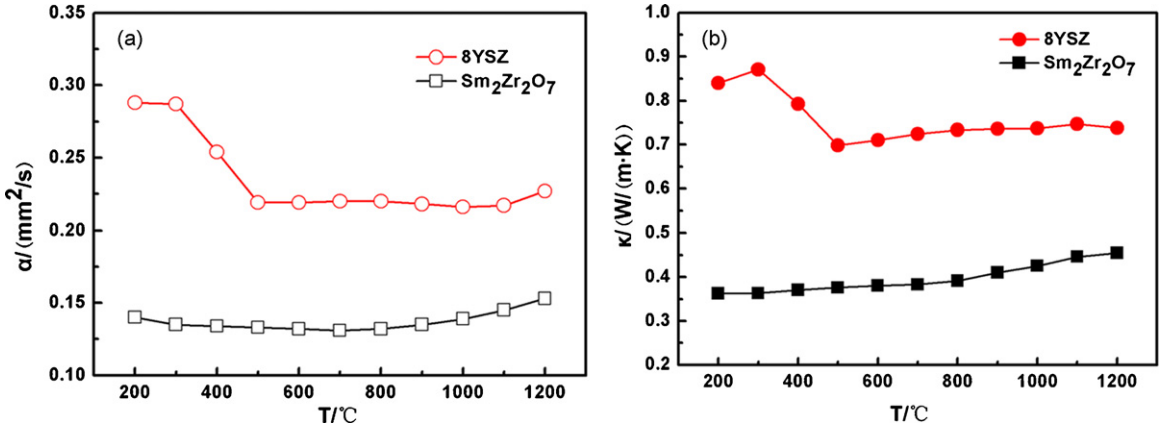

Fig. 5. (a) Thermal diffusivity and (b) thermal conductivity of $Sm_2Zr_2O_7$ and 8YSZ coatings.

gested a rather constant value up to 900 °C, and then followed by an increase at higher temperatures. The decrease in thermal conductivity means that a phonon conduction behavior is dominant in these polycrystalline materials,[22] while the increase in thermal diffusivity at relatively high temperatures is mainly attributed to initial sintering effects, because significant changes in microstructure are occurring at temperatures as low as 600 °C for plasma sprayed coatings due to microcrack healing and changes in shapes of inter-splat pores.[23]

The comparison of the values of calculated thermal conductivities of SZ and 8YSZ coatings (in Fig. 5b) suggests that the former in the range of 0.36–0.46 W/(m K) is much lower than the latter (0.70–0.87 W/(m K)).

Apart from the contribution of the microstructure, the lower thermal conductivity of SZ coatings can be attributed to the intrinsic factors. The thermal conductivity for a crystalline solid is due to changes of lattice vibrations, which are usually described in terms of phonons. The expression of the thermal conductivity is derived by Debye described as[24]:

$$\kappa = \frac{1}{3}\iota_p C_v \nu_m \tag{2}$$

where C_v is the specific heat, ν is the phonon velocity and ι_p is the mean free path for scattering of phonons.

The actual values of thermal conductivity depend sensitively on the defects such as vacancies and solutes which are strong phonon scatterers influencing ι_p. In SZ the defect chemistry due to co-doping can be represented using the Kröger–Vink notation by the equation,[25]

$$Sm_2O_3 \xrightarrow{ZrO_2} 2Sm_{Zr}' + V_O^{\bullet\bullet} + 3O_O^{\times} \tag{3}$$

where Sm_{Zr}' represents an Sm^{3+} cation that occupies a Zr^{4+} cation site, $V_O^{\bullet\bullet}$ is a doubly charged (positive) oxygen vacancy, and $O_O^{\times}$ is an O^{2-} anion on an oxygen site (neutral charge).

The effect of point defects on the phonon mean free path ι_p is given by Klemens[7] as follows:

$$\frac{1}{\iota_p} = \frac{\alpha^3}{4\pi\nu^4}\omega^4 c\left(\frac{\Delta M}{M}\right)^2 \tag{4}$$

where α^3 is the volume per atom, ν the transverse wave speed, ω the phonon frequency, c the defect concentration per atom, M the average mass of the host atom, $M + \Delta M$ the average mass of the solute atom, and for vacancies, the value of $\Delta M/M$ is calculated by:

$$\frac{\Delta M}{M} = \frac{M_\alpha}{2} - 2 \tag{5}$$

where M is the average mass per atom, M_α is the mass of the missing atom, and the term -2 accounts for the potential energy of the missing linkages, or twice the potential energy per atom.

The concentration (c) of oxygen vacancy in SZ is much higher than that in 8YSZ. Moreover, the atom masses of Sm, Y and Zr are 150.4, 88.9 and 91.2, respectively, the average atomic mass difference ($|\Delta M|$) between the solute (Sm) and host atom (Zr) is larger than that between Y and Zr, which contributes to higher effective phonon scattering by Sm solute cations in SZ than that of Y cations in 8YSZ. Therefore, the reduction in thermal conductivity of SZ is more obvious than that in 8YSZ.

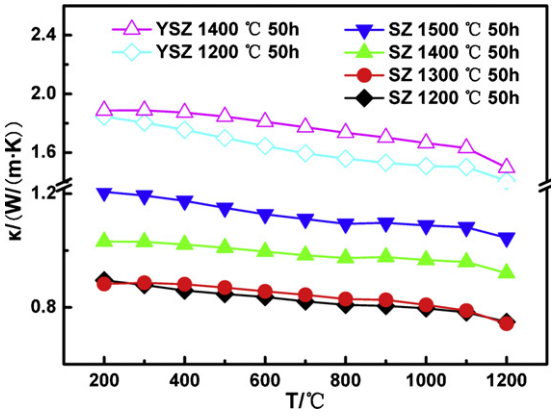

Fig. 6. Thermal conductivities of SZ and 8YSZ coatings heat treated at different temperatures for 50 h.

Thermal conductivity values of SZ and 8YSZ coatings after high temperature exposure for 50 h are shown in Fig. 6. Compared with the as-sprayed coatings, the thermal conductivities of coatings after heat treatment were considerably higher for both coatings. With the temperature increase in heat treatment, the thermal conductivities of both coatings increased substantially. However, after heat exposure at 1200 °C and 1400 °C for 50 h, thermal conductivities at 800 °C of SZ coatings were still ~48% and 44% lower than those of the 8YSZ coatings which were heat treated under the same conditions. It was reported that the thermal conductivity of plasma sprayed coatings was mainly determined by the real inter-splat contact area.[25] It is observed (in Fig. 3) that the exposure to high temperatures for an extended period leads to the growth of inter-splat contact area for coatings, which contributes to the significantly increase in thermal conductivities for SZ and 8YSZ coatings after heat treatment.

4. Conclusions

The phase stability, microstructure, heat transfer property of SZ coatings were investigated. For comparison, the thermal conductivities of plasma sprayed 8YSZ coatings were also studied under the same conditions. The following conclusions can be drawn from this work:

(1) A typical layered structure of plasma sprayed coatings was observed in these coatings, and the thinner individual splats in the SZ coating contributed to its lower thermal conductivity compared with 8YSZ coatings.
(2) The high quenching rate of plasma spraying produced a defect-fluorite phase in the as-sprayed SZ coating which transforms to the pyrochlore structure after heat treatment at temperatures above 1200 °C.
(3) The thermal diffusivities of SZ and 8YSZ coatings decreased initially, followed by an increase with further temperature rise which may be due to sintering effects during the measurement, the conductivity of as-sprayed SZ coatings was much lower than that of 8YSZ coatings even after

heat treatments due to the microstructure, high content of oxygen vacancy and large difference of atomic weight in SZ. The thermal conductivities of both coatings increased with the increase in heat treatment temperature due to the growth of real inter-splat contact area caused by sintering effects.

Acknowledgements

The authors would like to thank Ms. W.J. Qian and Mr. W. Wu for the SEM observations. We also express our appreciation to Mr. A. Cai, Miss C.Y. Luo and Mr. X.Y. Zhou for the thermal diffusivity measurement. Acknowledgement is also given to Mr. Z.J. Yin for his helpful comments.

References

[1]. Padture, N. P., Gell, M. and Jordan, E. H., Thermal barrier coatings for gas-turbine engine applications. *Science*, 2002, **296**, 280–284.

[2]. Miller, R. A., Current status of thermal barrier coatings: an overview. *Surf. Coat. Technol.*, 1987, **30**, 1–11.

[3]. Stiger, M. J., Yanar, N. M., Topping, M. G., Pettit, F. S. and Meier, G. H., Thermal barrier coatings for the 21st century. *Z. Metallkd.*, 1999, **90**, 1069–1078.

[4]. Sodeoka, S., Suzuki, M., Inoue, T., Ueno, K. and Oki, S., Thermal spray practical solutions for engineering problems. In *Proceedings of the 9th National Thermal Spray Conference*, ed. C. C. Berndt. ASM International, Materials Park, Ohio, 1996, pp. 295–302.

[5]. Stöver, D., Pracht, G., Lehmann, H., Dietrich, M., Döring, J.-E. and Vaβsen, R., New material concepts for the next generation of plasma-sprayed thermal barrier coatings. *J. Therm. Spray Technol.*, 2004, **13**, 76–83.

[6]. Thornton, J. and Majumdar, A., Ceria precipitation and phase stability in zirconia based thermal barrier coatings. In *Proceedings of the 14th International Thermal Spray Conference*, ed. A. Ohmori. ASM International, Kobe, Japan, 1995, pp. 1075–1080.

[7]. Klemens, P. G., Phonon scattering by oxygen vacancies in ceramics. *Physica B*, 1999, **263-264**, 102–104.

[8]. Clarker, D. R. and Phillpot, S. R., Thermal barrier coating materials. *Mater. Today*, 2005, **8**, 22–29.

[9]. Wu, J., Novel low-thermal-conductivity ceramics for thermal barrier coating applications. PhD thesis. University of Connecticut; 2004.

[10]. Cao, X. Q., *Thermal Barrier Coating Materials*. The Publishing House of Science, Beijing, 2007.

[11]. Liu, Z. G., Ouyang, J. H. and Zhou, Y., Structural evolution and thermophysical properties of $(Sm_xGd_{1-x})_2Zr_2O_7$ $(0 \leq x \leq 1.0)$ ceramics. *J. Alloys Compd.*, 2009, **472**, 319–324.

[12]. Zhao, H. B., Levi, C. G. and Wadley, H. N. G., Vapor deposited samarium zirconate thermal barrier coatings. *Surf. Coat. Technol.*, 2009, **203**, 3157–3167.

[13]. Swalin, R. A., *Thermodynamics of Solids*. Wiley, New York, 1972, pp. 53–87.

[14]. Kubaschewsji, O., Alcock, C. B. and Spencer, P. J., *Materials Thermochemistry* (*6th ed.*). Pergamon Press, Oxford, 1993, pp. 257–323.

[15]. Paul, S., Cipitria, A., Golosnoy, I. O., Xie, L., Dorfman, M. R. and Clyne, T. W., Effects of impurity content on the sintering characteristics of plasma-sprayed zirconia. *J. Therm. Spray Technol.*, 2007, **16**, 798–803.

[16]. Soltani, R., Coyle, T. W., Mostaghimi, J., Lima, R. S. and Moreau, C., Thermo-physical properties of plasma sprayed yttria stabilized zirconia coatings. *Surf. Coat. Technol.*, 2008, **202**, 3954–3959.

[17]. Sampath, S. and Herman, H., Rapid solidification and microstructure development during plasma spray deposition. *J. Therm. Spray Technol.*, 1996, **5**, 445–456.

[18]. Mandal, B. P. and Tyagi, A. K., Preparation and high temperature-XRD studies on a pyrochlore series with the general composition $Gd_{2-x}Nd_xZr_2O_7$. *J. Alloys Compd.*, 2007, **437**, 260–263.

[19]. Wang, C., Zinkevich, M. and Aldinger, F., Experimental investigation and thermodynamic modeling of ZrO_2–$SmO_{1.5}$ system. *J. Am. Soc.*, 2007, **90**, 2210–2219.

[20]. Duran, P., Phase relationships in the hafnia–gadolinia system. *Ceramurgia Int.*, 1977, **3**, 137–140.

[21]. Pannetier, J., Energie electrostatique des reseaux pyrochlore. *J. Phys. Chem. Solids*, 1973, **34**, 583–589.

[22]. Youngblood, G. E., Rice, R. W. and Ingel, R. P., Thermal diffusivity of partially and fully stabilized (yttria) zirconia single crystals. *J. Am. Ceram. Soc.*, 1988, **71**, 255–260.

[23]. Ilavsky, J., Long, G. G., Allen, A. J. and Berndt, C. C., Evolution of the void structure in plasma-sprayed YSZ deposits during heating. *Mater. Sci. Eng. A*, 1999, **272**, 215–221.

[24]. Xi, T. G., *Thermophysical Properties of Inorganic Materials*. Shanghai Scientific and Technical Press, Shanghai, 1981 [in Chinese].

[25]. McPherson, R., A model for the thermal conductivity of plasma sprayed ceramic coatings. *Thin Solid films*, 1984, **112**, 89–95.